applied sciences

MDPI

Article

Development of Heavy Metal Potentiostat for Batik Industry

Siti Nur Hanisah Umar [1], Mohammad Nishat Akhtar [1], Elmi Abu Bakar [1,*], Noorfazreena M. Kamaruddin [1] and Abdul Rahim Othman [2]

[1] School of Aerospace Engineering, Engineering Campus, Universiti Sains Malaysia, Nibong Tebal 14600, Penang, Malaysia; snhanisahumar@gmail.com (S.N.H.U.); nishat@usm.my (M.N.A.); fazreena@usm.my (N.M.K.)

[2] Department of Mechanical Engineering, Universiti Teknologi PETRONAS, Seri Iskandar 32610, Perak, Malaysia; rahim.othman@utp.edu.my

* Correspondence: meelmi@usm.my

Received: 31 August 2020; Accepted: 5 October 2020; Published: 4 November 2020

Abstract: The consumption of reactive dyes in the batik industry has led to a severe concern in monitoring the heavy metal level in wastewater. Due to the necessity of implementing a wastewater monitoring system in the batik factory, a Heavy Metal potentiostat (HMstat) was designed. The main goal of this study is to understand the optimal design concept of the potentiostat function in order to investigate the losses of accuracy in measurement using off-the-shelf devices. Through lab-scale design, the HMstat comprises of an analog potentiostat read-out circuit component (PRCC) and a digital control signal component (CSC). The PRCC is based on easy to use components integrated with a NI-myRIO controller in a CSC. Here, the myRIO was equipped with built-in analog to digital converter (ADC) and digital to analog converter (DAC) components. In this paper, the accuracy test and detection of cadmium(II) (Cd^{2+}) and lead(II) (Pb^{2+}) were conducted using the HMstat. The results were compared with the Rodeostat (an open source potentiostat available on the online market). The accuracy of the HMStat was higher than 95% and within the precision rate of the components used. The HMstat was able to detect Cd^{2+} and Pb^{2+} at −0.25 and −0.3 V, respectively. Similar potential peaks were obtained using Rodeostat (Cd^{2+} at −0.25 V and Pb^{2+} at −0.3 V).

Keywords: potentiostat; heavy metal; cadmium; lead; batik; Rodeostat

1. Introduction and background

Batik is a traditional handmade textile craft in the cottage industry [1]. This industry has contributed positively to economic growth, especially in Kelantan and Terengganu in Malaysia, and has also become one of the main attractions of foreign and local tourists [2]. Batik factories are known to generate a large amount of wastewater included wax, resin, sodium, silicate, and dyes. The presence of dyes is one of the main concerns in wastewater [3]. Among all types of dyes, reactive dyes are preferred due to their convenience, transparency, and brilliant color along with ease of textile fastening [4].

Five different types of reactive dyes were studied in [5], and the results reported that each reactive dye contains heavy metal elements of cadmium (Cd), lead (Pb), arsenic (As), zinc (Zn), chromium (Cr), cobalt (Co), and copper (Cu). Amongst all, Zn and Cr are essential elements, and small doses are required by living organisms to maintain various biochemical and physiological functions [6–9], while the others are non-essential elements which are highly toxic and harmful to human health and the environment, even at low concentrations [6,7].

According to the Environmental Quality Act (EQA 1974), the permissible limit for industrial effluent discharge based on standard A (applicable to discharge into any inland waters within catchment

areas) for Cd is 0.01 ppm, As and Cr are 0.05 ppm, Pb is 0.1 ppm, Cu is 0.2 ppm, and Zn is 1.0 ppm [10]. However, as most of the batik factories were build-up with improper or without a waste management system, the level of heavy metals discharged was not determined [11]. This happened due to the lack of awareness regarding the hazardous effect of heavy metal elements toward the environment and especially concerning human health [11].

Determination of the heavy metal level before being discharged to the environmental water is crucial. Today, various heavy metal detection techniques have been established, including inductive coupled plasma mass spectrometry (ICP-MS), inductively coupled plasma atomic emission spectrometry (ICP-AES), inductively coupled plasma-optical emission spectrometry (ICP-OES), atomic absorption spectrometry (AAS), atomic emission spectrometry (AES) [12], X-ray Fluorescence Spectrometry (XRF), cold vapor atomic absorption spectrometer (CVAAS), neutron activation analysis (NAA), and flameless atomic absorption spectrophotometry (FAAS) [12–14]. These techniques are highly sensitive and selective [14]. However, these techniques are inconvenient for fieldwork application, such as in a batik factory, because instruments are relatively expensive, bulky, require complex operational procedures, and long detection times [12–14].

Nowadays, electrochemical techniques hold great potential to realize the on-field detection of heavy metal elements in the batik factory. This technique has the advantages of low-cost, ease of operation, fast analysis, and is also well suited to fabricate on a small circuit for portable and on-field application [12–15]. Until now, numerous research has been done in the development of electrochemical devices for various applications, which are known as potentiostats [16–23].

One of the potentiostat developments is an Arduino-based potentiostat, fabricated using inexpensive components which were capable of performing simple electrochemical experiments and were suitable for an undergraduate teaching level [17–19]. For such experiments, the results and data were recorded in real-time on a Windows-based computing system via a USB interface [17]. However, a potentiostat integrated with Raspberry Pi eliminated the requirement of an external computing system. This standalone device carried out the electrochemical experiments, and the results were displayed on an LCD touch panel [20]. Both Arduino- and Raspberry Pi-based potentiostats did not possess a built-in analog to digital converter (ADC), and digital to analog converter (DAC) and the requirement for external ADC and DAC made the design more complicated.

Many previous works have reported on the capability of a self-fabricated potentiostat to detect heavy metal elements. A potentiostat named CheapStat [21] was capable of detecting the arsenic (As) level in lake water. The test was conducted using a gold disk working electrode (WE), a platinum counter electrode (CE), and a silver/silver-chloride (Ag/AgCl) reference electrode (RE). A universal mobile electrochemical detector (UMED) [16] is a potentiostat which is compatible with a mobile phone and is capable of detecting cadmium (Cd), lead (Pb), and zinc (Zn). A screen-printed electrode (SPE) was used with UWED, which consists of carbon ink modified by carbon nanotubes as a WE, carbon ink as a CE, and Ag/AgCl ink as a RE. A programmable system on chip (PSoC) [22] is a commercially available integrated circuit (IC) that does not require any external electronic components to perform electrochemical experiments. The PSoC demonstrated the detection of Pb using gold wire as a WE and Ag/AgCl as a CE and RE. The latest work reported was a MiniStat [23], in which the design was developed to be suited for general electrochemical analysis in the smaller form factor. The MiniStat was tested to detect copper (Cu) using a 3 mm glassy carbon WE, a platinum wire as a CE, and Ag/AgCl as a RE. However, the potentiostats mentioned previously [16,21,23] demand the user to fabricate a printed circuit board (PCB) and to solder the electronic components onto the board. Since these potentiostats were designed with small surface-mounted integrated circuits (ICs), they required more skilled technicians and sophisticated tools to solder together, as compared to through-hole connections. This creates hindrances to chemists and other scientists who want to use a potentiostat.

Besides, the detecting heavy metal as reported in [21–24] used a three separated electrodes approach which is bulky and not suited for on-field application. The incorporation of a screen-printed electrode (SPE) eliminated the classical bulky electrodes and at the same time, enabled reduction in the

sample used [25]. Although there are several reports working on modified SPE and WE [16,25–28], since heavy metals have defined redox potential, the selectivity toward specific heavy metal ions still can be achieved by bare electrodes and unmodified SPE [29].

Therefore, in the requirement of a heavy metal feature-based device for monitoring heavy metal levels in the batik industry, a Heavy Metal Potentiostat device (HMstat) incorporated with SPE was designed. The design of HMstat was based on the idea to simplify the potentiostat design by implementing a controller equipped with built-in DAC and ADC. With this, the development of electronic components in the potentiostat focused more on the main part, which is the potential control and current measurement part. Besides, the construction of the electronic component in HMstat implemented through-hole technology, which eliminates the hindrance for users who are less skilled in electronic areas in designing a potentiostat. Moreover, implementing through-hole technology enabled the design to be easily adjusted or replaced when necessary. This study will also demonstrate the capability of HMstat to implement performance tests and heavy metal measurements.

2. Methodology

2.1. Design of HMstat

The HMstat consists of two main components, which comprise of the digital control signal component (CSC) and the electronic component, which is the analog potentiostat read-out circuit component (PRCC), as shown in Figure 1. The function of the CSC is for parameter control, signal generation, acquisition, and processing. The CSC is based on NI myRIO, which is equipped with built-in ADC and DAC provided with a bipolar input/output voltage channel up to ±10 V. These features allow the reduction in stages in PRCC from nine steps (from previous work [19]) to three steps (for this current work; refer to Figure 2). The stages in PRCC can be categorized into two parts, which are the potential control part (PCP) and the current measurement part (CMP). There are two stages in PCP; the first stage consists of a summing inverting amplifier (AO_{SUM}), and the second stage is a voltage follower (AO_F). The function of the PCP is to apply and control the interfacial potential at the WE through CE with the consideration of feedback potential from the RE through AO_F (the function of AO_F is to limit any current that might otherwise flow through RE [30]). Thus, the applied potential input to the electrochemical cell can be expressed using Equation (1):

$$V_{in} = \frac{R_2}{R_1} V_{ap}, \tag{1}$$

where V_{ap} is the applied potential generated by CSC; R_1 and R_2 are resistor 1 and resistor 2, respectively. Since $R_1 = R_2 = 10\ k\Omega$, thus ideally, V_{in} applied to the electrochemical cell will be equal to the V_{ap}.

Here, the CMP is comprised of a transimpedance amplifier (OA_{TIA}) with the function to covert the small current changed from the electrochemical cell to a voltage signal. The correlation between the measured current change and the output voltage from OA_{TIA} can be expressed using Equation (2):

$$I_{out} = \frac{V_{out}}{R_{gain}}, \tag{2}$$

where I_{out} is the measured output current, V_{out} is the output voltage, and R_{gain} is the gain resistor of OA_{TIA} with a resistance value of 10 kΩ.

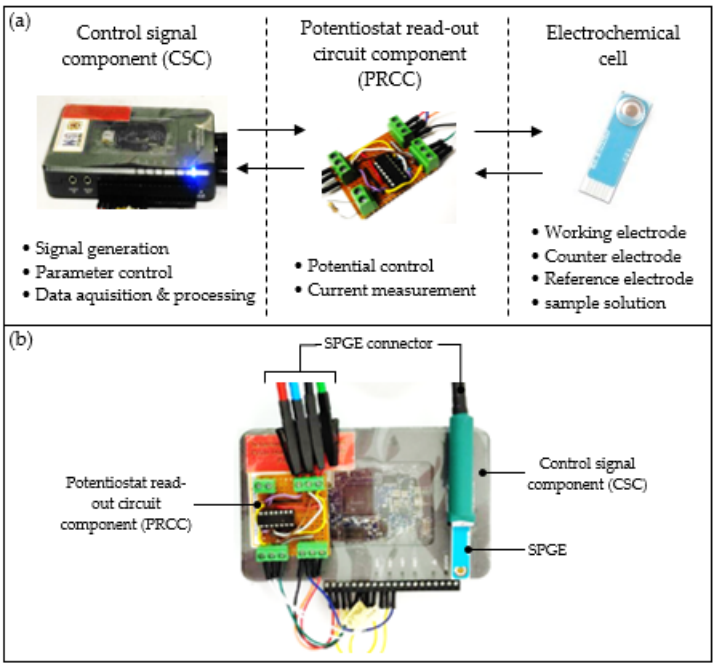

Figure 1. (**a**) The HMstat consists of a control signal component (CSC) and potentiostat read-out circuit component (PRCC) connected to the electrochemical cell (consisting of a screen-printed electrode gold (SPGE)) and (**b**) overall connection of HMstat.

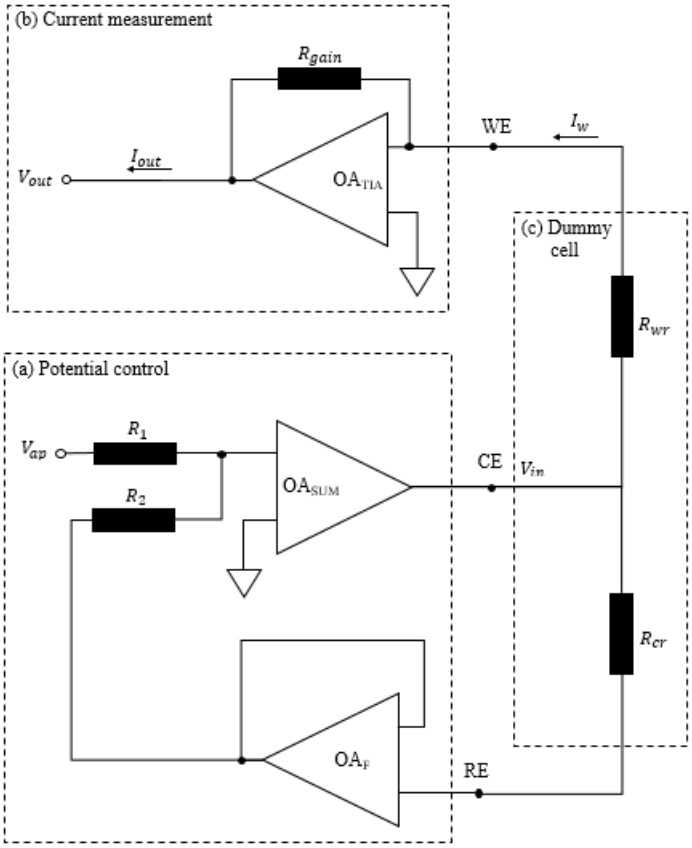

Figure 2. Block diagram of the potentiostat read-out circuit component (PRCC) comprised of (**a**) potential control part (PCP) and (**b**) current measurement part (CMP), connected to a (**c**) dummy cell (for accuracy and noise measurement).

2.2. Signal Generation and Processing

The HMstat has been designed in such a way that it can perform two types of measurement. One is the measurement for performance tests, and the second is for heavy metal measurement. Three different types of signals were designed for the performance test, which were the constant potential, ramp potential, and square wave potential. For heavy metal measurement, a square wave anodic stripping voltammetry (SWASV) signal was designed. Basically, the SWASV signal is the incorporation of the constant, ramp, and square wave potential signal.

These signals were generated and configured in the CSC using graphical programming language. The development of the graphical programs is depicted in the flowchart, as illustrated in Figure 3. Based on the figure, once the program has been turned on, the user must choose to perform the performance test or heavy metal measurement test. If the performance test is chosen, the user must set the performance test parameters and then, press the "Start performance test" button. The generated V_{ap} is applied to the PRCC by a mini system port (MSP) through analog output zero (AO0) and then, the performance test is implemented. At the same time, the data acquisition of $V_{in(m)}$ and $V_{out(m)}$ is to be done from the PRCC through MSP analog input zero (AI0) and one (AI1), respectively. Once the test is finished, the data are saved as xlsx file. In addition, the test can be aborted at any moment by pressing the "Stop test" button. Meanwhile, if heavy metal measurement is chosen, the user will undergo a similar sequence as done for the performance test.

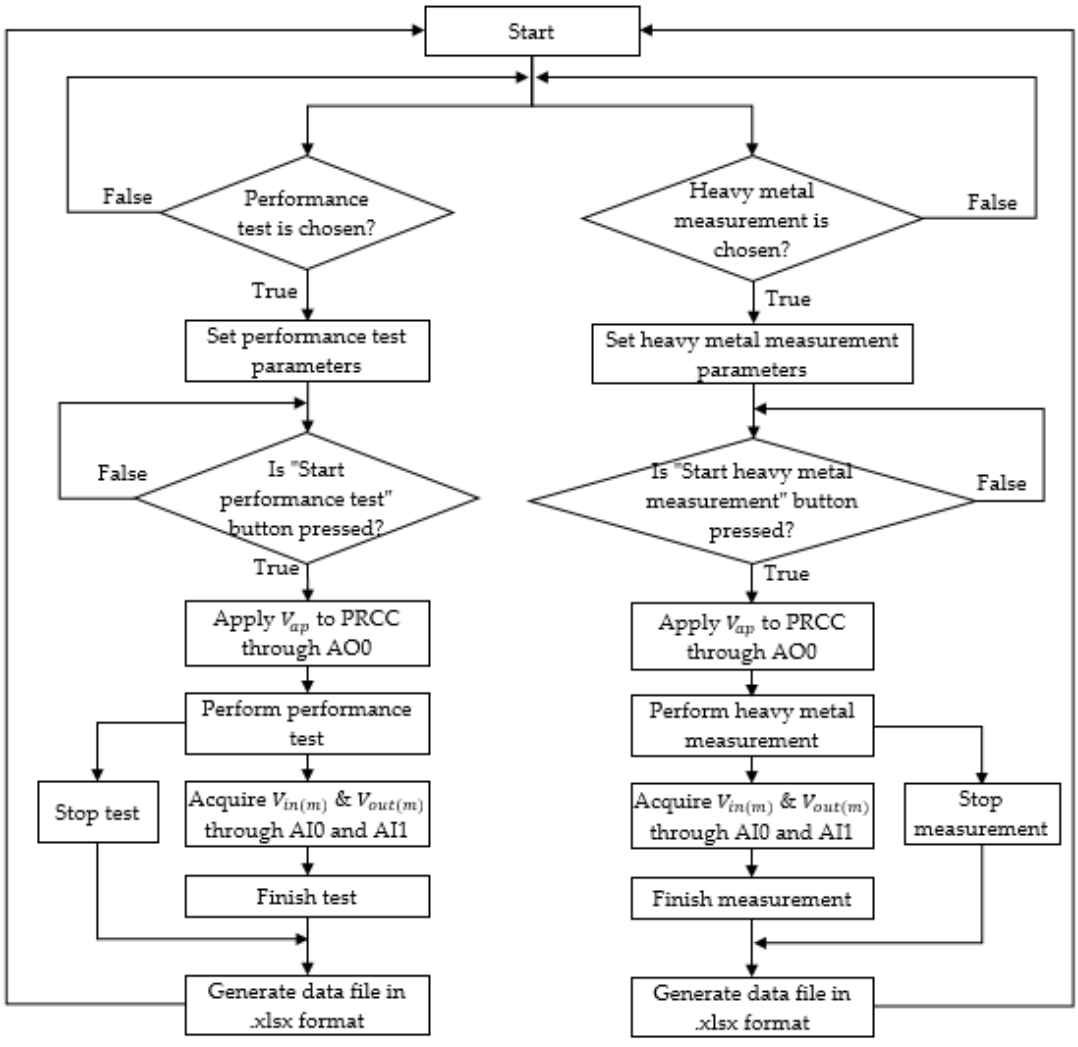

Figure 3. Flow chart of graphical program for signal generation (apply potential, V_{in}) and acquisition (measured input potential, $V_{in(m)}$ and measured output potential, $V_{out(m)}$).

2.3. Accuracy and Noise Measurement of HMstat

The HMstat performance test was conducted to evaluate: (1) the capability of the PCP to accurately apply the desired potential to WE, (2) the accuracy of the CMP to measure the operating current I_w, and (3) the noise current measurement of the CMP under operating current I_w. To assess the performance of the HMstat, a dummy cell was designed and connected to the CE, WE, and RE of the HMstat. The dummy cell (refer to Figure 2c) is an electronic circuit used to replicate the primary electrochemical cell with a known operating current I_w.

As mentioned earlier, three types of V_{ap} (constant, ramp, and square wave potential) were used for the HMstat performance test. Under a different kind of V_{ap}, the accuracy of the PCP and CMP was measured based on the percentage error (PE), as given in the following equations:

$$Accuracy\ of\ PCP = 100 - PE_{PCP} \tag{3}$$

$$Accuracy\ of\ CMP = 100 - PE_{CMP} \tag{4}$$

where PE_{PCP} and PE_{CMP} are the percentage error of the PCP and CMP, respectively, calculated using Equations (5) and (6).

$$PE_{PCP} = \left| \frac{V_{in(m)} - V_{ap}}{V_{ap}} \right| \times 100, \tag{5}$$

$$PE_{CMP} = \left| \frac{I_{out} - I_w}{I_w} \right| \times 100, \tag{6}$$

where $V_{in(m)}$ is the measured V_{in} taken through AI0, I_{out} is the measured output current taken through AI1, and I_w is the current flow through R_{wr}.

Here, the noise current measurement of the CMP was taken as the standard deviation of the data [22,30,31].

The performance of the HMstat was then compared to another available potentiostat in the online market, which is the Rodeostat (Rstat). The availability of the Rstat, which was tested under different types of V_{ap}, was shown in Table 1.

Table 1. Type of potential applied to the HMstat and Rstat.

Type of V_{ap}	V_{ap} (V)	Test Part	Parameter	HMstat	Rodeostat
Constant	−0.5	PCP	V_{in}	√	×
		CMP	I_{out}	√	√
	+0.5	PCP	V_{in}	√	×
		CMP	I_{out}	√	√
Ramp	−1 to +1	PCP	V_{in}	√	×
		CMP	I_{out}	√	√
SWV	−1 to +1	PCP	V_{in}	√	×
		CMP	I_{out}	√	×

√ tested; × not tested due to the data unavailability.

2.4. Detection of Heavy Metal Using Square Wave Anodic Stripping Voltammetry Method

In this study, the capability of the HMstat to detect heavy metal elements was demonstrated. The working solution of 10 ppm of Pb and Cd was prepared by diluting a standard solution of Pb and Cd (1000 ppm) in 0.1 M acetate buffer. The screen-printed gold electrodes (SPGEs) were purchased from DropSens (Spain). Each strip contained three electrodes printed on the same planar platform. The three electrodes were a 4 mm diameter gold disk-shaped working electrode (WE), a gold counter electrode (CE), and a silver pseudo-reference electrode (RE). All detection was performed by placing

100 µL solution on the three-electrode strip. It is to be noted that all the potential applied throughout this work refers to silver pseudo-RE.

The experiment was conducted using a square wave anodic stripping voltammetry method (SWASV), in which the SWASV signal was generated by the CSC. There were two main steps in the SWASV method. First was the deposition step and second was the stripping step. The mechanism of the heavy metal ion during the deposition and stripping steps was illustrated in Figure 4. The deposition step is where the negative potential is applied to the WE. The purpose of the deposition step was to reduce the heavy metal ion in the working solution onto the electrode surface. The reduction will occur if the applied deposition potential is more negative than the reduction potential of heavy metal [32]. This step was followed by the stripping step. In the stripping step, the deposited heavy metal ion on the electrode surface is reoxidized and dissolved into the working solution [32]. The reoxidation tends to occur when the applied potential matches the oxidation potential of each heavy metal, so that the measured current indicates a different peak for each heavy metal species [16]. The details of the parameters used in the steps for heavy metal ion detection were listed in Table 2.

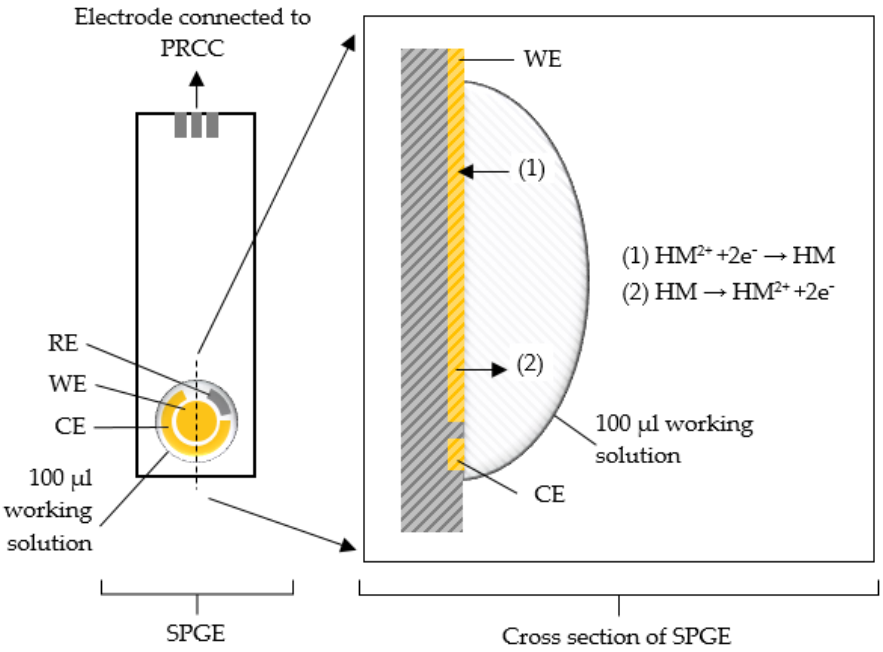

Figure 4. Heavy metal (HM) ion during (1) deposition and (2) stripping step on screen-printed gold electrode (SPGE) connected to potentiostat read-out circuit component (PRCC). RE, WE, and CE are reference electrode, working electrode, and counter electrode, respectively.

Table 2. Experimental parameters.

Deposition Step	
Potential	−0.9 V
Time	120 s
Stripping Step	
Initial potential	−0.7 V
Final potential	0.0 V
Modulation amplitude	50 mV
Step amplitude	50 mV
frequency	10 Hz

3. Results and Discussion

3.1. Accuracy and Noise Measurement

Based on Equations (5) and (6), the percentage error (PE) of the PCP and CMP of the HMstat, and the CMP of Rstat was shown in Figure 5. The PE obtained by the HMstat for both PCP and CMP was less than 5% for every types of V_{ap}. Generally, the lowest error was observed when the V_{ap} was at the constant potential. The highest error was obtained for the ramp potential followed by SWV potential. The constant potential produced significantly lower error compared to the ramp and SWV. This was due to the fluctuated signal of the ramp and SWV, which may have led to higher noise generation. Moreover, these patterns were also observed in the PE of the CMP for Rstat. However, the PE obtained for the CMP of the Rstat was higher compared to HMstat for all types of V_{ap}.

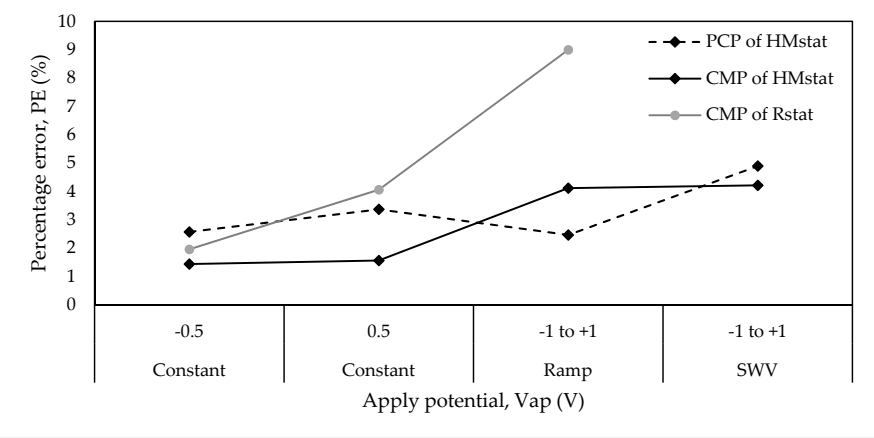

Figure 5. Accuracy of the current measurement part (CMP) for HMstat and Rstat.

Table 3 shows the performance HMstat and Rstat, including the lists of PE, accuracy, and noise measurement. The accuracy was measured based on Equations (3) and (4) and the noise measurement was determined based on the standard deviation of the data. The measurement of the accuracy was related to PE, and the accuracy of HMstat was higher than 95% which is within the precision rate of the components used. Moreover, HMstat showed better accuracy compared to Rstat in a similar pattern as in PE. The degradation of accuracy might have been caused by a higher noise current, as V_{ap} changed from constant potential to ramp potential, and to SWV. The lowest noise current was obtained for constant V_{ap} (5 nA for both V_{ap} of −0.5 V and +0.5 V). The noise current increased to 6 nA when ramp V_{ap} was applied. The highest noise current of 7 nA has been obtained for SWV V_{ap}. This was due to the fluctuated signal of ramp, and SWV, which may have led to higher noise generation.

Table 3. Performance of HMstat and Rodeostat (Rstat) in term of percentage error (PE), accuracy, and noise current measurement (SD).

Type of V_{ap}	V_{ap} (V)	Potentiostat	PE (%)		Accuracy (%)		SD (μA)
			PCP	CMP	PCP	CMP	SD
Constant	−0.5	HMstat	2.575	1.445	97.425	98.555	5.215
		Rstat	×	1.961	×	98.039	6.934 μ
	+0.5	HMstat	3.373	1.567	96.627	98.433	5.337
		Rstat	×	4.063	×	95.937	14.364 μ
Ramp	−1 to +1	HMstat	2.470	4.121	97.530	95.879	6.789
		Rstat	×	8.998	×	91.002	20.664 μ
SWV	−1 to +1	HMstat	4.899	4.219	95.101	95.781	7.287
		Rstat	×	×	×	×	×

× not tested due to the data not being able to be obtained.

3.2. Heavy Metal Detection Test

Figure 6a shows the stripping peak of 10 ppm Cd^{2+} and 10 ppm Pb^{2+}. Based on the figure, the Cd^{2+} and Pb^{2+} stripping peaks were observed at −0.30 and −0.25 V, respectively, and the peaks were located quite close to each other. This was due to the fact that detection was done using a gold-based electrode. With regard to this, there were several studies which reported that closer stripping peaks were observed for Cd^{2+} and Pb^{2+} under gold-based electrodes and the presence of both metals in the solution caused overlapping of the stripping peaks [33–35]. Moreover, the presence of Cd^{2+} in Pb^{2+} measurements will affect the stripping intensity of Pb^{2+} and vice versa [33]. Figure 6b shows the stripping peaks of Cd^{2+} and Pb^{2+} extracted from [34] were close to each other and simultaneous detection of Pb^{2+} and Cd^{2+} will cause overlapping of the stripping peaks.

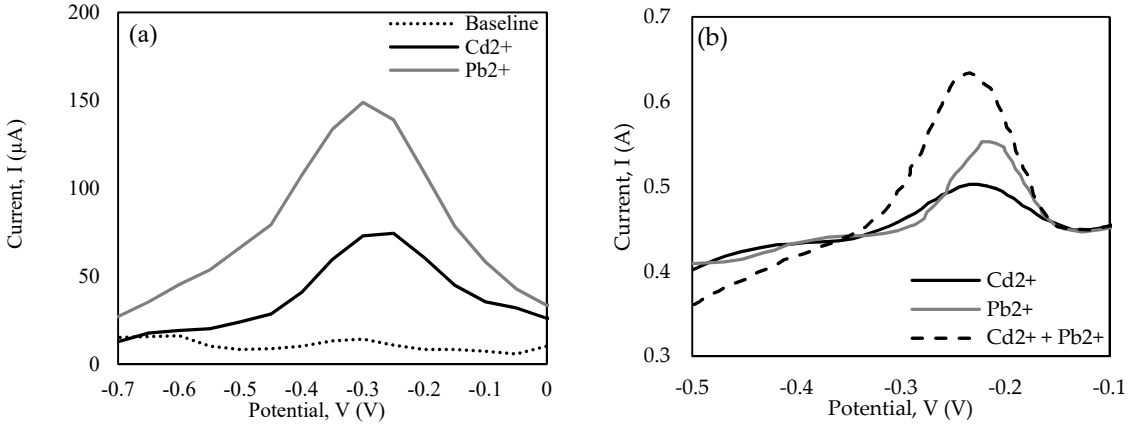

Figure 6. (**a**) Stripping peak of Cd^{2+} and Pb^{2+} using HMstat incorporated with a screen-printed gold electrode (SPGE). Experimental condition: deposition potential −0.6 V; deposition time 120 s; modulation and step amplitude 50 mV and frequency 10 Hz. In 0.1 M acetate buffer. (**b**) Stripping peak of Cd^{2+} (at −0.195 V) and Pb^{2+} (at −0.18 V) under gold-based electrode, extracted from previous research [34].

Figure 6a also shows that the current intensity of the Cd^{2+} stripping peak versus Pb^{2+} was significantly smaller, in which the peak current of Cd^{2+} was 74 μA and the peak current of Pb^{2+} was 148 μA. This indicated that the HMstat has higher sensitivity to detect Pb^{2+} compared to Cd^{2+}. Similar results were also observed in [35] and as shown in Figure 6b [34], where the peak current of Pb^{2+} obtained was more elevated than Cd^{2+}.

The same experimental procedures were repeated using Rstat. The detection results of HMstat were compared with Rstat. Referring to Figure 7, using Rstat, the stripping peak of Cd^{2+} and Pb^{2+} were located at −0.25 and −0.3 V, respectively. These results were the same when compared to HMstat. As expected, the peak current of the Pb^{2+} using Rstat and HMstat was quite similar (136 and 148 μA for Rstat and HMstat, respectively). However, the peak current of Cd^{2+} (297 μA) using Rstat showed significantly higher value when compared to the result obtained by the HMstat. It was also observed that using Rstat, the peak current of Cd^{2+} was higher when compared to the Pb peak, which indicated that Rstat has a higher sensitivity to detect Cd^{2+} when compared to Pb^{2+}. This result is in contradiction with the result obtained in [35] and in Figure 6b [34].

Based on the above results, the stripping peak of simultaneous detection of Cd^{2+} and Pb^{2+} under gold-based electrode using both HMstat and Rstat interfered with each other's peaks. This can be overcome by electrode modification to improve anti-interference of the electrode by diminishing either one stripping peak [36], or by implementing a chemometrics method such as back-propagation artificial neural network (BP-ANN) using the formation of a prediction model for detection Cd^{2+} and Pb^{2+} [37].

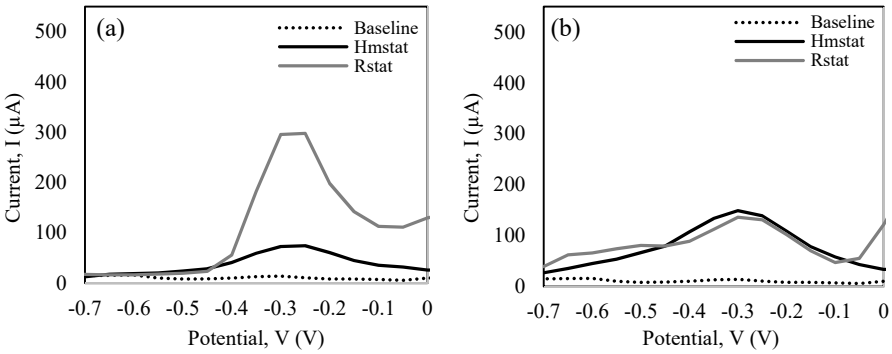

Figure 7. Comparison detection peak between HMstat and Rodeostat (Rstat) for (**a**) Cd^{2+} and (**b**) Pb^{2+}. Using the same experimental condition as in Figure 6.

4. Conclusions

The novel idea to design and optimize the performance of the potentiostat apparatus called HMstat is based on easy to use components integrated with a NI myRIO equipped with built-in ADC and DAC units; thus, making the overall design of the HMstat less complicated and easy to handle and operate. With respect to the methodological function of the proposed apparatus pertaining to its reliability, noise measurement, accuracy tests, and heavy metal detection tests were conducted. The noise measurement of the HMstat was lower than 7 nA, and the accuracy of the HMstat was higher than 95%, which indicated that the HMstat is within the precision rate of the component used. The detection result showed that the HMstat was capable of detecting Cd^{2+} and Pb^{2+} at a stripping peak of 0.25 and −0.3 V, respectively. Through investigation, the significant potential peak of Cd^{2+} and Pb^{2+} had agreement with slight overlapping under a gold-based electrode, as shown in the above result.

Furthermore, the simultaneous detection of Cd^{2+} and Pb^{2+} or detection of a single element of Cd^{2+} in the presence of Pb^{2+} or vice versa will be more challenging in the near future, as the locations of the stripping peaks of Cd^{2+} and Pb^{2+} were close to each other and tend to overlap and affect each other. It was also observed that the HMstat had higher sensitivity to detect Pb^{2+} compared to Cd^{2+}. This was based on the intensity current of the Pb^{2+} stripping peak, which was significantly higher compared to Cd^{2+}.

Author Contributions: Conceptualization, S.N.H.U. and E.A.B.; Formal analysis, M.N.A.; Funding acquisition, E.A.B. and A.R.O.; Methodology, S.N.H.U., E.A.B. and N.M.K.; Project administration, E.A.B.; Supervision, M.N.A. and N.M.K.; Writing—original draft, S.N.H.U.; Writing—review and editing, M.N.A. and A.R.O. All authors have read and agreed to the published version of the manuscript.

Funding: The authors would like to acknowledge the RU Top-Down research grant (1001/PAERO/870052), (1001/PAERO/6740041) provided by the Research Creativity and Management Office, Universiti Sains Malaysia to support this research. The authors would also like to acknowledge the Research Management Office of Universiti Teknologi Petronas and its industrial grant (015MD0-052) for supporting this research.

Acknowledgments: The proposed experiments have been carried out in the School of Aerospace Engineering of Universiti Sains Malaysia. The authors would also like to acknowledge the Ministry of Education (MOE) Malaysia for supporting S.N.H.U. under Universiti Sains Malaysia Academic Staff Training Scheme (ASTS).

Conflicts of Interest: The authors declare that they have no known competing financial interests or personal relationships that could have appeared to influence the work reported in this paper.

References

1. Subki, N.S.; Hashim, R.; Muslim, N.Z.M. Heavy metals adsorption by pineapple wastes activated carbon: KOH and $ZnCl_2$ activation. *AIP Conf. Proc.* **2019**, *2068*, 020035. [CrossRef]
2. Ahmad, A.L.; Harris, W.A.; Syafiie, S.; Ooi, B.S. Removal of Dye From Wastewater of Textile Industry Using Membrane Technology. *J. Teknol.* **2002**, *36*, 31–44. [CrossRef]
3. Rashidi, H.R.; Sulaiman, N.M.N.; Hashim, N.A.; Hassan, C.R.C.; Ramli, M.R. Synthetic reactive dye wastewater treatment by using nano-membrane filtration. *Desalin. Water Treat.* **2015**, *55*, 86–95. [CrossRef]

4. World Batik Council Types of Batik. Available online: http://www.worldbatikcouncil.com/batikhistory/typesofbatik.htm (accessed on 6 April 2020).
5. Reddy, S.; Osborne, W.J. Biocatalysis and Agricultural Biotechnology Heavy metal determination and aquatic toxicity evaluation of textile dyes and effluents using Artemia salina. *Biocatal. Agric. Biotechnol.* **2020**, *25*, 101574. [CrossRef]
6. Jaishankar, M.; Tseten, T.; Anbalagan, N.; Mathew, B.B.; Beeregowda, K.N. Toxicity, mechanism and health effects of some heavy metals. *Interdiscip. Toxicol.* **2014**, *7*, 60–72. [CrossRef]
7. Turdean, G.L. Design and Development of Biosensors for the Detection of Heavy Metal Toxicity. *Int. J. Electrochem.* **2011**, *2011*, 1–15. [CrossRef]
8. Hashim, R.; Song, T.H.; Muslim, N.Z.M.; Yen, T.P. Determination of heavy metal levels in fishes from the lower reach of the kelantan river, Kelantan, Malaysia. *Trop. Life Sci. Res.* **2014**, *25*, 21–39. [CrossRef]
9. Pirsaheb, M.; Fattahi, N.; Sharafi, K.; Khamotian, R.; Atafar, Z. Essential and toxic heavy metals in cereals and agricultural products marketed in Kermanshah, Iran, and human health risk assessment. *Food Addit. Contam. Part B Surveill.* **2016**, *9*, 15–20. [CrossRef]
10. Government Printing Office. *Environmental Quality (Sewage and Industrial Effluents) Regulations, 1979*; Government Printing Office: Putrajaya, Malaysia, 1979.
11. Sajab, M.S.; Ismail, N.N.N.; Santanaraj, J.; Mohammad, A.W.; Hassan, H.A.; Chia, C.H.; Zakaria, S.; Noor, A.M. Insight observation into rapid discoloration of batik textile effluent by in situ formations of zero valent iron. *Sains Malays.* **2019**, *48*, 393–399. [CrossRef]
12. Zukri, M.N.M.; Bakar, E.A.; Mohamed-Kassim, Z. An Electroanalytical Instrument Equipped with Wireless Communication Network and Graphical User Interface for Real-time Monitoring Wastewater Status from Batik Industry. *J. Mech. Eng.* **2017**, *4*, 153–170.
13. Bansod, B.K.; Kumar, T.; Thakur, R.; Rana, S.; Singh, I. A review on various electrochemical techniques for heavy metal ions detection with different sensing platforms. *Biosens. Bioelectron.* **2017**, *94*, 443–455. [CrossRef] [PubMed]
14. Lu, Y.; Liang, X.; Niyungeko, C.; Zhou, J.; Xu, J.; Tian, G. A review of the identification and detection of heavy metal ions in the environment by voltammetry. *Talanta* **2018**, *178*, 324–338. [CrossRef] [PubMed]
15. Lv, Z.-L.; Qi, G.-M.; Jiang, T.-J.; Guo, Z.; Yu, D.-Y.; Liu, J.-H.; Huang, X.-J. A simplified electrochemical instrument equipped with automated flow-injection system and network communication technology for remote online monitoring of heavy metal ions. *J. Electroanal. Chem.* **2017**, *791*, 49–55. [CrossRef]
16. Nemiroski, A.; Christodouleas, D.C.; Hennek, J.W.; Kumar, A.A.; Maxwell, E.J.; Fernandez-Abedul, M.T.; Whitesides, G.M. Universal mobile electrochemical detector designed for use in resource-limited applications. *Proc. Natl. Acad. Sci. USA* **2014**, *111*, 11984–11989. [CrossRef] [PubMed]
17. Meloni, G.N. Building a Microcontroller Based Potentiostat: A Inexpensive and Versatile Platform for Teaching Electrochemistry and Instrumentation. *J. Chem. Educ.* **2016**, *93*, 1320–1322. [CrossRef]
18. Li, Y.C.; Melenbrink, E.L.; Cordonier, G.J.; Boggs, C.; Khan, A.; Isaac, M.K.; Nkhonjera, L.K.; Bahati, D.; Billinge, S.J.; Haile, S.M.; et al. An Easily Fabricated Low-Cost Potentiostat Coupled with User-Friendly Software for Introducing Students to Electrochemical Reactions and Electroanalytical Techniques. *J. Chem. Educ.* **2018**, *95*, 1658–1661. [CrossRef]
19. Umar, S.N.H.; Bakar, E.A.; Kamaruddin, N.M.; Uchiyama, N. A Low Cost Potentiostat Device For Monitoring Aqueous Solution. *MATEC Web Conf.* **2018**, *217*, 8. [CrossRef]
20. Agata, T.N.; Uzuki, K.S. Building a Low-cost Standalone Electrochemical Instrument Based on a Credit Card-sized Computer. *Anal. Sci.* **2018**, *34*, 1109. [CrossRef]
21. Rowe, A.A.; Bonham, A.J.; White, R.J.; Zimmer, M.P.; Yadgar, R.J.; Hobza, T.M.; Honea, J.W.; Ben-Yaacov, I.; Plaxco, K.W. CheapStat: An Open-Source, "Do-It-Yourself" Potentiostat for Analytical and Educational Applications. *PLoS ONE* **2011**, *6*, e23783. [CrossRef]
22. Lopin, P.; Lopin, K.V. PSoC-Stat: A single chip open source potentiostat based on a Programmable System on a Chip. *PLoS ONE* **2018**, *13*, e0201353. [CrossRef]
23. Adams, S.; Doeven, E.H.; Quayle, K.; Kouzani, A. MiniStat: Development and evaluation of a mini-potentiostat for electrochemical measurements. *IEEE Access* **2019**, *7*, 31903–31912. [CrossRef]

24. Umar, S.N.H.; Abu Bakar, E.; Kamaruddin, N.M.; Uchiyama, N. A Prototype Development and Evaluation of Electrochemical Device for Heavy Metal Measurement. In *Lecture Notes in Mechanical Engineering of International Conference of Aerospace and Mechanical Engineering 2019*; Springer: Berlin/Heidelberg, Germany, 2019; pp. 117–125.
25. Barton, J.; García, M.B.G.; Santos, D.H.; Fanjul-Bolado, P.; Ribotti, A.; McCaul, M.; Diamond, D.; Magni, P. Screen-printed electrodes for environmental monitoring of heavy metal ions: A review. *Microchim. Acta* **2016**, *183*, 503–517. [CrossRef]
26. Kim, J.; Campbell, A.S.; de Ávila, B.E.F.; Wang, J. Wearable biosensors for healthcare monitoring. *Nat. Biotechnol.* **2019**, *37*, 389–406. [CrossRef] [PubMed]
27. Dai, Y.; Liu, C.C. Recent Advances on Electrochemical Biosensing Strategies toward Universal Point-of-Care Systems. *Angew. Chem.-Int. Ed.* **2019**, *58*, 12355–12368. [CrossRef]
28. Biyani, M.; Biyani, R.; Tsuchihashi, T.; Takamura, Y.; Ushijima, H.; Tamiya, E.; Biyani, M. DEP-On-gO for simultaneous sensing of multiple heavy metals pollutants in environmental samples. *Sensors* **2017**, *17*, 45. [CrossRef]
29. Li, M.; Gou, H.; Al-Ogaidi, I.; Wu, N. Nanostructured sensors for detection of heavy metals: A review. *ACS Sustain. Chem. Eng.* **2013**, *1*, 713–723. [CrossRef]
30. Dryden, M.D.M.M.; Wheeler, A.R. DStat: A Versatile, Open-Source Potentiostat for Electroanalysis and Integration. *PLoS ONE* **2015**, *10*, e0140349. [CrossRef]
31. Hoilett, O.S.; Walker, J.F.; Balash, B.M.; Jaras, N.J.; Boppana, S.; Linnes, J.C. Kickstat: A coin-sized potentiostat for high-resolution electrochemical analysis. *Sensors* **2020**, *20*, 2407. [CrossRef]
32. Rajendran, P.; Musfirah, N.; Anjang, A.; Rahman, A.; Razak, N.A. *Lecture Notes in Mechanical Engineering of International Conference of Aerospace and Mechanical Engineering 2019*; Springer: Berlin/Heidelberg, Germany, 2019; ISBN 9789811547553.
33. Bernalte, E.; Arévalo, S.; Pérez-Taborda, J.; Wenk, J.; Estrela, P.; Avila, A.; Di Lorenzo, M. Rapid and on-site simultaneous electrochemical detection of copper, lead and mercury in the Amazon river. *Sens. Actuators B Chem.* **2020**, *307*, 127620. [CrossRef]
34. Noh, M.F.M.; Tothill, I.E. Development and characterisation of disposable gold electrodes, and their use for lead(II) analysis. *Anal. Bioanal. Chem.* **2006**, *386*, 2095–2106. [CrossRef]
35. Laschi, S.; Palchetti, I.; Mascini, M. Gold-based screen-printed sensor for detection of trace lead. *Sens. Actuators B Chem.* **2006**, *114*, 460–465. [CrossRef]
36. Zhao, G.; Wang, H.; Liu, G. Direct quantification of Cd2+ in the presence of Cu2+ by a combination of anodic stripping voltammetry using a Bi-film-modified glassy carbon electrode and an artificial neural network. *Sensors* **2017**, *17*, 1558. [CrossRef]
37. Zhao, G.; Liu, G. Interference Effects of Cu(II) and Pb(II) on the Stripping Voltammetric Detection of Cd(II): Improvement in the Detection Precision and Interference Correction. *J. Electrochem. Soc.* **2018**, *165*, H488–H495. [CrossRef]